CHEMISTRY
A EUROPEAN JOURNAL

DOI: 10.1002/chem.200801784

pH-Dependent Optical Properties of Synthetic Fluorescent Imidazoles

Mikhail Y. Berezin,[a] Jeff Kao,[b] and Samuel Achilefu*[a, c]

Abstract: An imidazole moiety is often found as an integral part of fluorophores in a variety of fluorescent proteins and many such proteins display pH-dependent light emission. In contrast, synthetic fluorescent compounds with incorporated imidazoles are rare and have not been studied as pH probes. In this report, the richness of imidazole optical properties, including pH sensitivity, was demonstrated by means of a novel imidazole-based fluorophore 1*H*-imidazol-5-yl-vinylbenz[*e*]indolium. Three species corresponding to protonated, neutral, and deprotonated imidazoles were identified in the broad range of pH 1–12. The absorption and emission bands of each species were assigned by comparative spectral analysis with synthesized mono- and di-*N*-methylated fluorescent imidazole analogues. pK_a analysis in the ground and the excited states showed photoacidic properties of the fluorescent imidazoles due to the excited state proton transfer (ESPT). This effect was negligible for substituted imidazoles. The assessment of a pH-sensitive center in the imidazole ring revealed the switching of the pH-sensitive centers from 1-N in the ground state to 3-N in the excited state. The effect was attributed to the unique kind of the excited state charge transfer (ESCT) resulting in a positive charge swapping between two nitrogens.

Keywords: charge transfer · emission spectroscopy · energy transfer · imidazole · pH sensitivity · sensors

Introduction

Fluorescent molecular pH sensors are widely used to control and monitor chemical reactions and biological processes. A majority of the available synthetic fluorescent probes employ tunable acidity of phenyls (napththols, fluoresceins, and pyranines) and cyclic aromatic amines (oxazoline, cyanines, and porphyrins)[1–5] to create pH-sensitive centers. Interestingly, fluorescent proteins with a seemingly limited choice of available pH-sensitive groups utilize mostly the same set of functionalities: phenyls,[6] aromatic amines,[7] and oxazoles.[8] However, in addition to common groups, some fluorescent proteins also employ imidazole as a pH-sensitive functionality (class 6 according to Tsien classification[9]). For example, imidazole is a key constituent of the fluorophore system of red fluorescent proteins EBFP2, mCherry, and EosFP,[7,10] (Figure 1) and apparently is responsible for their pH sensitivity.[11–13] To the best of our knowledge, there have been no reports on utilizing imidazole moieties in synthetic pH probes despite the attractive optical properties of imidazole-containing fluorophores, such as high quantum yield and pH dependence.

The long standing interest of our laboratory lies in synthesis of novel near-infrared probes and their applications in biological imaging. Recently, we initiated a screening of organic functionalities which could be suitable as pH sensors and synthetically appropriate for incorporation into a polymethine skeleton. Here, inspired by the optical properties of fluorescent proteins, we report our first experimental data where the new molecular construct was based on incorporating an imidazole heterocycle via a methine linker into a fluorogenic π-conjugated benz[*e*]indolium core (compound **2**, see Scheme 1). Optical studies on the synthesized molecules revealed a number of interesting and sometimes unexpected observations. We noted three modes of pH sensitivity in the range of pH 1–12 attributed to the protonated, neutral, and deprotonated forms of imidazole with different degrees of

[a] Dr. M. Y. Berezin, Prof. Dr. S. Achilefu
Department of Radiology, Washington University School of Medicine
4525 Scott Avenue, St. Louis, MO 63110 (USA)
Fax: (+1) 314-747-5191
Homepage: http:/www/orl.wustl.edu
E-mail: achilefus@mir.wustl.edu

[b] Dr. J. Kao
Department of Chemistry, Washington University
St. Louis, MO 63130 (USA)

[c] Prof. Dr. S. Achilefu
Department of Biochemistry & Molecular Biophysics
Washington University School of Medicine, St. Louis, MO 63110 (USA)

Supporting information for this article is available on the WWW under http://dx.doi.org/10.1002/chem.200801784.

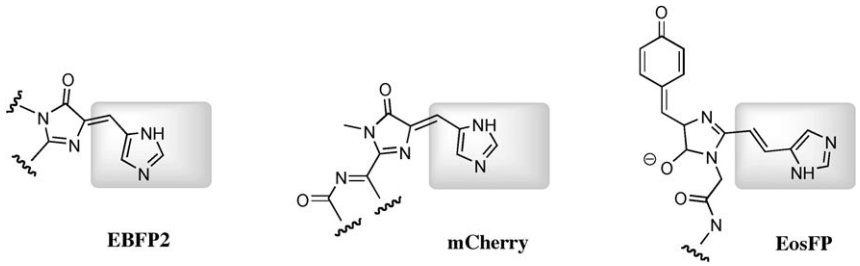

Figure 1. Fluorophores from red-emitting proteins: mCherry,[7] EBFP2,[7] and EosFP.[10]

fluorescence. There existed at least two channels of the excited state charge transfer (ESCT) at certain pH: within the imidazole ring and between the imidazole ring and benz[*e*]indolium. The interpretation of pH sensitivities in both ground and excited states and the detailed investigation of the related underlying mechanisms were the goals of this study.

Results and Discussion

Synthesis of fluorescent imidazoles: To understand the mechanism of pH sensitivity, we prepared imidazole **2** and examined its optical properties and compared them with related compounds such as di-*N*-methylated imidazolium **3** and mono-*N*-methylated imidazoles **4** and **5**, an approach often used in the literature to explore the mechanism of protonation.[14–16] Fluorescent imidazoles **2–4** were prepared by electrophilic substitution by mixing imidazole-bearing aldehydes prepared in our laboratory[17] or from commercial sources with a known fluorophore building block 3-(2-carboxyethyl)-1,1,2-trimethyl-1*H*-benz[*e*]indolium (**1**; Scheme 1). The pendant carboxylate group in **1** was selected for potential further conjugation with bioactive molecules.[4] With a stoichiometric ratio of the starting materials, the conversion was nearly quantitative. Compounds **2**, **4**, and **5** were made as internal salts from the pairing of a carboxylate ion with the positively charged benzoindolium; compound **3** is a BF_4^+ salt.[17]

While imidazoles **2**, **3**, and **4** could be easily made from commercially or readily available imidazole carbaldehydes,[17] the preparation of 3-*N*-methylimidazole **5** presented a certain challenge due to the lack of regioselective imidazole methylation at the 3-N position. Our initial efforts based on literature methods led to a mixture of isomers[18] or required protection–deprotection schemes,[19,20] which resulted in lower yields. Finally, we chose methylation of 5-imidazole carbaldehyde with a stoichiometric amount of methyl iodide. The mixture of 1-*N* methyl and 3-*N* methyl derivatives (ratio 2:3, ^{1}H NMR spectroscopy) was found to be difficult to separate. After the aqueous workup, the mixture was allowed to react with benz[*e*]indolium **1** via electrophilic substitution in the next step. The reaction mixture containing two products with the same molecular masses was easily separated into two constituent compounds by reversed-phase chromatography. The ^{1}H NMR and LCMS spectra of the first, more hydrophilic elutant were identical to the compound alternatively prepared from commercially available 1-*N*-methylimidazole carbaldehyde. The second, more hydrophobic product, is most likely the 3-*N*-methylimidazole isomer **5**.

To confirm their identity, compounds **4** and **5** were fully characterized by ^{1}H and ^{13}C NMR spectroscopy, including COSY, HMQC, and HMBC. The final assignment of an *N*-methyl group position was made by ^{1}H NOE experiments (Figure 2 and the Supporting Information). Irradiation of compound **4** at $\delta = 4.17$ ppm (H-16) led to the observed signal enhancements of the two nearest protons, H-12 ($\delta =$ 8.18 ppm) and H-15 ($\delta = 8.92$ ppm), confirming that the methyl group was attached to the 1-N position. In contrast, irradiation at $\delta = 3.89$ ppm (H-16) of the second elutant resulted in the enhancement of H-14 ($\delta = 8.05$ ppm) and H-15 ($\delta = 8.22$ ppm), suggesting that the methyl group is connected to the 3-N position and confirming that the second elutant is 3-*N*-methyl-substituted regioisomer **5.** In addition, the strong NOE between H-12 and H-9 (not shown) and the absence of a NOE between H-14 and H-12 (crossed dotted arrow) indicated a *trans–cis* conformation of compound **4**. In contrast, a strong NOE between H-12 and H-9 (not shown) and a strong NOE between H-14 and H-12 (dotted arrow) indicated *trans–trans* conformation of **5.**[21]

Absorption and emission spectra assignment: For the analysis of pH-dependent properties, the spectra were recorded in water between pH 1.0 and 12.0 using diluted HCl or NaOH for pH adjustment. At pH 6, compound **2** showed a broad absorption band at 430 nm and a smaller band at 360 nm (Figure 3, left). At lower pH, the absorption of the visible band became smaller with a simultaneous increase of the near-UV band with a diffuse isosbestic point at 370 nm. Below pH 2.9, the 360 nm band became dominant

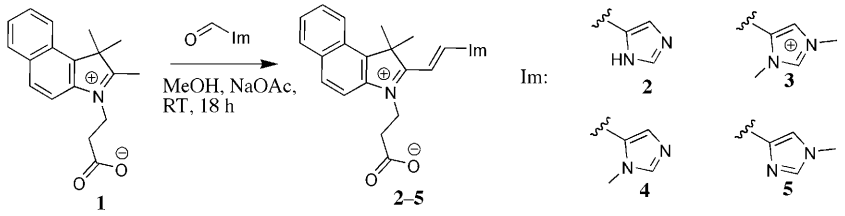

Scheme 1. Synthesis of imidazole(Im)-containing fluorophores.

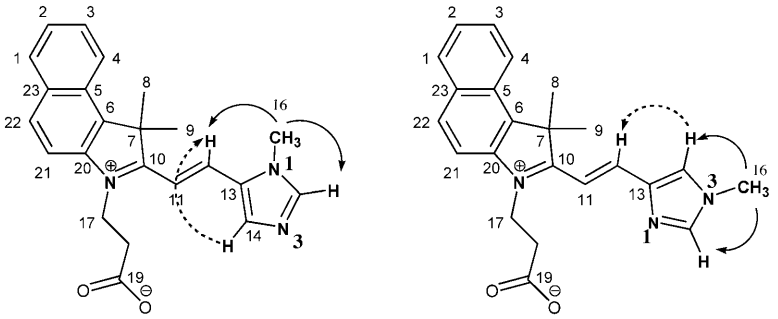

4 **5**

Figure 2. Interactions between protons used to assign the position of the methyl group by NOE. ^{1}H NOE enhancement: **4** (left): $\delta = 4.17$ ppm to $\delta = 8.18$ and 8.92 ppm: H-16 to H-12 and H-15; **5** (right): $\delta = 3.89$ ppm to $\delta = 8.05$ and 8.22 ppm: H-16 to H-14 and H-15.

of two titration centers and therefore the presence of the three states, which we tentatively assigned as the protonated, neutral, and deprotonated forms of imidazole (Scheme 2).

In an acidic environment, compound **2** revealed a broad and almost structureless fluorescence at 600 nm (Figure 4, left). Under neutral conditions, the fluorescence became much weaker and blue-shifted to 560 nm with an isoemissive point at 525 nm. Further basification increased the emission intensity upon excitation at 460 nm, accompanied by a pronounced emission shift to 530 nm (Figure 4, right). The change in absorbance and emission titration curves as a function of pH revealed three well-separated regions in both the ground and excited states (Figure 5). Optical properties of the compounds under acidic, neutral, and basic conditions are given in Table 1.

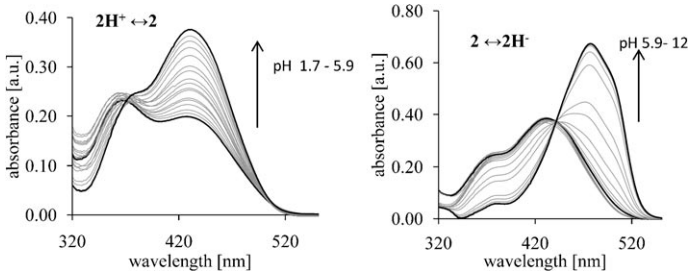

Figure 3. Absorption spectra of **2** under acidic (left) and basic (right) conditions in water. Absorbance increases with the increase of pH and shifts to longer wavelengths.

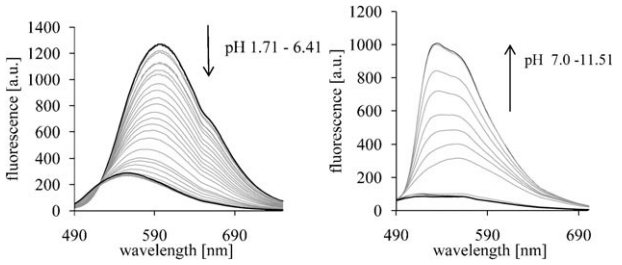

Figure 4. Fluorescence spectra of compound **2** at pH from 1.7 to 6.4 (left, excitation 400 nm) and at pH 7.0–11.51 (right, excitation 460 nm).

and no further changes in absorption band were observed past pH 2.5. Under basic conditions, the absorption band experienced a red shift to 477 nm with a well-defined isosbestic point at 440 nm (Figure 3, right). The presence of two independent isosbestic points clearly suggested the existence

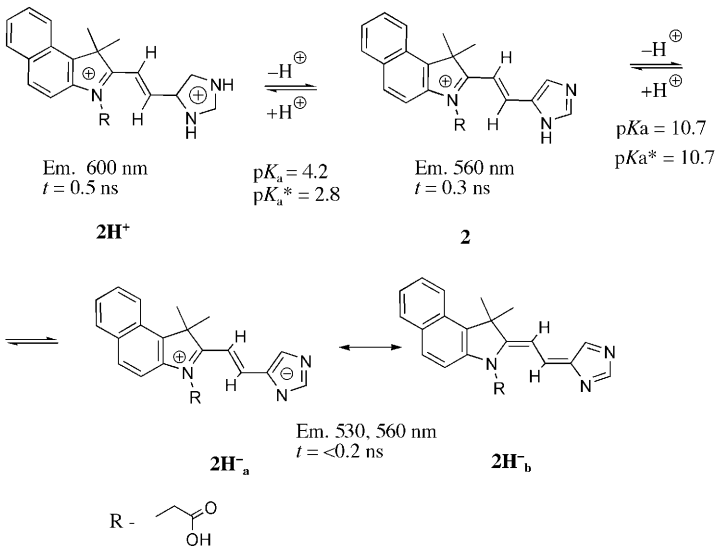

Scheme 2. Suggested transformations of **2** under acidic, neutral, and basic conditions. pK_a and pK_a* were determined for the ground and excited states, respectively.

All species showed similar molar absorptivity values at a given pH and exhibited a general upward trend with an increase in pH (from 9000–16 000 $M^{-1}cm^{-1}$ in acidic solutions to 21 000–25 500 $M^{-1}cm^{-1}$ in basic media, Table 1). Similarly, all compounds exhibited large and pH-dependent Stokes shifts (ca. 11 000 cm^{-1} at pH 2, ca. 5000 cm^{-1} at pH 7, and ca. 2000 cm^{-1} at pH 11). Quantum yields and fluorescence lifetimes for the studied molecules were rather low in water but

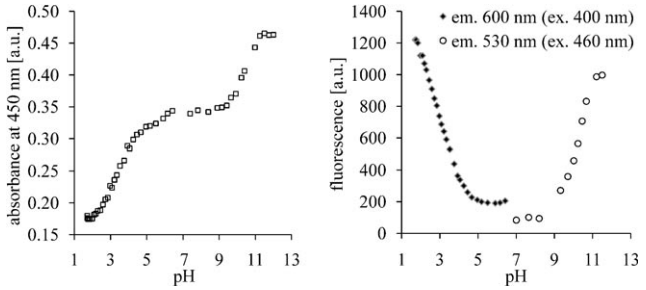

Figure 5. Titration absorption spectra of compound **2** (left) and titration emission spectra (right, excitation and emission as indicated).

Table 1. Molar absorptivities and quantum yields of compounds **2–5** in water at different pH.[a]

Entry	pH 2		pH 7		pH 11	
	ε [$M^{-1}cm^{-1}$]	Φ[b,f]	ε [$M^{-1}cm^{-1}$]	Φ[c,f]	ε [$M^{-1}cm^{-1}$]	Φ[c,d]
2	9200	0.014	15400	0.002	25500	0.004
3	16000	0.006	15500[e]	0.008[e]	degradation	
4	11400	0.008	15300	0.001	21000	n/f[g]
5	12100	0.013	15100	0.002	21100	n/f

[a] ε: molar absorptivity obtained at max absorption wavelength. [b] Excitation at 400 nm. [c] Excitation at 460 nm. [d] Quantum yield Φ relative to fluorescein in 0.1 N NaOH. [e] pH 6.2, at higher pH, significant decomposition has been observed. [f] Quantum yield Φ relative to quinine in 0.1 M H_2SO_4. [g] n/f: non-fluorescent.

significantly increased in a constrained environment, such as highly viscous media, which typically exist inside proteins. Indeed, relatively weak fluorescence of **2** in aqueous solutions with a fluorescence quantum yield $\Phi = 0.014$ and lifetime $\tau = 0.5$ ns increased significantly to $\Phi = 0.15$, $\tau = 1.19$–1.28 ns in glycerol.

Acidic and neutral media: To assign absorption and emission bands, we first considered acidic and neutral conditions. Compound **3**, which was previously synthesized in our laboratory[10] and possesses a permanent cationic charge set due to the exhaustive *N*-methylation of imidazole, was used as an isoelectronic analogue of the protonated imidazolium $\mathbf{2H^+}$. As expected, **3** was not pH sensitive (no spectral shift in acidic and neutral pH, Figure 6), which correlated well

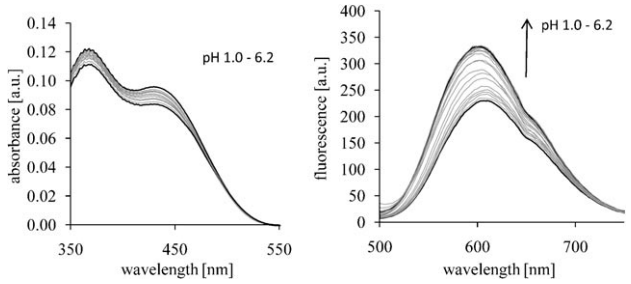

Figure 6. Absorption and emission spectra of **3** under acidic and neutral conditions in water (excitation 400 nm). The overall change in quantum yield for compound **3** was less than 30%.

with the lack of "active solvation centers"[22] in the molecule. The change in molar absorptivity and quantum yield of **3** from neutral to acidic pH was much smaller than the corresponding changes in compound **2** (Table 1). The absorption and the emission spectra of the compound $\mathbf{2H^+}$ in acidic media and of **3** in both acidic and neutral solutions clearly resembled each other, suggesting electronic similarity between the two entities. Fluorescence lifetime measurements of $\mathbf{2H^+}$ and **3** showed that both molecules had the same lifetime of 0.5 ns. The similarities of the spectral parameters (position, shape, and lifetime) of $\mathbf{2H^+}$ and **3** suggested that the absorption at 360 nm and emission at 600 nm band belonged to the protonated imidazolium $\mathbf{2H^+}$ (Scheme 2). In the fluorescence spectra of **3**, the absence of the band at 560 nm in spectra for **2** and $\mathbf{2H^-}$ under the neutral and basic conditions correlated well with the absence of the neutral form of **3**. Thus, the emission at 560 nm in neutral pH of **2** was unequivocally assigned to the neutral imidazole (Scheme 2).*Basic media*: Having assigned protonated and neutral forms, we turned our attention to compound **2** under basic conditions ($\mathbf{2H^-}$). At a pH greater than 9, the absorption spectra showed a dramatic change, which was characterized by a red shift to 477 nm and a significant increase in absorption intensity (Figure 3, right). Simultaneously, the fluorescence experienced a substantial blue shift to 530 nm (Figure 4, right). These changes were unique to **2** among the four studied imidazoles and were attributed to the formation of the imidazole anion $\mathbf{2H^-_a}$ or its resonance form $\mathbf{2H^-_b}$ via the deprotonation of the imidazole ring (Scheme 2). Unlike **2**, the absorption spectra of compounds lacking labile N–H protons such as **4** and **5** under basic conditions showed no bathochromic shifts and no new isosbestic points (Figure 8), suggesting the absence of the respective deprotonated forms. Indeed, the absorption spectra of **4** and **5** under basic conditions were similar to the absorption spectra of the neutral imidazole **2** (Figure 3 and Figure 8). Also the absence of blue-shifted fluorescent peaks under basic conditions for **4** and **5** at 530 nm (Figure 9) further supported the absence of deprotonation for these molecules. Thus, the 477 nm band in the absorption spectra of **2** was assigned to their deprotonated forms $\mathbf{2H^-_{a,b}}$.

The pK_a of the $\mathbf{2} \leftrightarrow \mathbf{2H^-}$ deprotonation in both the ground state and the excited state was determined to be 10.7. Such a pK_a value is unusually low for imidazoles since the deprotonation of imidazoles to their anionic form, imidazolates, is typically higher ($pK_a = 14.5$[23]) and necessitates very strong bases. However, in the presence of certain functionalities, the pK_a can be lowered significantly. For example, the presence of electron-withdrawing groups might shift the dissociation constant to lower pK_a values; that is, for urocanic acid, a pK_a value of 13[20] has been observed. Furthermore, conjugation of the imidazolate ring to a positively charged group (e.g. benz[*e*]indolium) can lower the pK_a even more due to the energetically favorable loss of overall charge and the formation of a neutral conjugated chromophore $\mathbf{2H^-_b}$ (a related case was recently described by Oto et al.[24]).

Among neutral, protonated, and deprotonated forms of **2**, the protonated form demonstrated the highest fluorescence (Table 1). The decrease of fluorescence and the blue shift from 600 nm to 530–560 nm (Figure 4) was apparently caused by photo-induced electron transfer originating from an unshared electron pair located in the imidazole nitrogens,[25] which is electronically coupled with a chromophore. Under acidic conditions, the electron pair was deactivated via protonation and did not compete with the radiative decay on the same level. For that reason, the emissions of the electronically identical $\mathbf{2H^+}$, di-*N*-methylated **3**, and mono-*N*-methylated protonated $\mathbf{4H^+}$ and $\mathbf{5H^+}$ were found to be quite similar (Figure 7); in all the structures the electron pair was blocked.

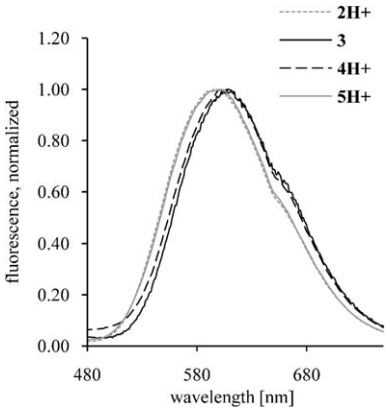

Figure 7. Normalized fluorescence spectra of compounds **2–5** at pH 2 (excitation 400 nm). Emission traces of $\mathbf{2H^+}$ and $\mathbf{5H^+}$ completely overlap. Emission traces of **3** and $\mathbf{4H^+}$ are shifted 7–8 nm.

Determination of the pH-sensitive nitrogen center—pK_a analysis: Having established the correlation between imidazole structures and their optical properties, we closely examined the behavior of the protonated molecules to establish which nitrogen in the imidazole ring of **2** is responsible for pH sensitivity. Careful analysis of Figure 7 revealed that, despite an obvious similarity in emission profiles between the studied imidazoliums, the emission profile of $\mathbf{2H^+}$ fully overlapped only with the emission of $\mathbf{5H^+}$, suggesting significant resemblance between these two excited species. In addition, detailed pK_a analysis showed that the sensitivities in the ground state and in the excited state were different: 1-N was the pH-sensitive center in the ground state and 3-N in the excited state.

The pK_a values of the studied compounds in the ground and excited states were determined from the corresponding absorption and emission spectra (Figure 3, 4, 8, and 9) by using principal component analysis (PCA), and were validated with sigmoidal dose-response curve fits (see the Supporting Information) from titration diagrams. The results are tabulated in Table 2.

Imidazole $\mathbf{2H^+}$ exhibited photoacidic properties, known as excited-state proton transfer (ESPT).[26–29] In the excited state, the pK_a was 1.4 pH units lower than the pK_a of the ground state. Calculated molar ratios for each of the principal components (from PCA) as a function of pH are shown in Figure 10. Each of the three panels represents a photolytic equilibrium of two principal components identified in the ground and the excited state. The point of the intersection of both components at each panel corresponds to the pK_a

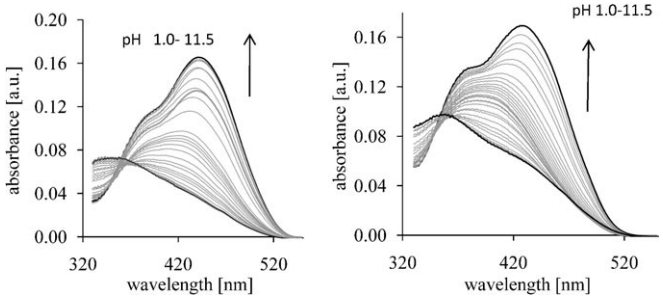

Figure 8. Absorption spectra of **4** (left) and **5** (right) at pH 1.0–11.5. Absorbance increases with increasing pH. The existence of only one isosbestic point suggests the presence of only two species: protonated and neutral forms.

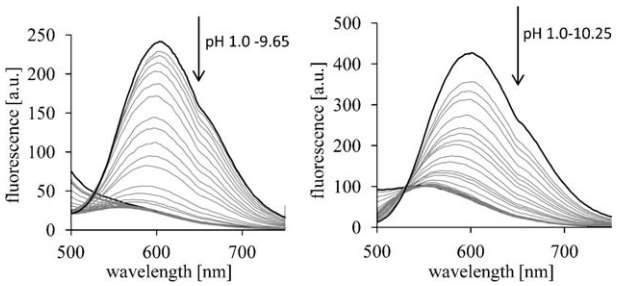

Figure 9. Fluorescence spectra of compounds **4** (left) and **5** (right) (excitation 400 nm). Fluorescence decreases with increasing pH and remains stable after pH 6. No emission signals at 530–560 nm at basic pH suggests the absence of deprotonated forms.

Table 2. pK_a of fluorescent imidazoles in acidic media in the ground and excited states, calculated from PCA and titration diagrams (in parenthesis).

	$\mathbf{2\leftrightarrow 2H^+}$	$\mathbf{4\leftrightarrow 4H^+}$	$\mathbf{5\leftrightarrow 5H^+}$
ground state, pK_a	4.20 (4.20 ± 0.05)	4.22 (4.39 ± 0.03)	2.68 (2.75 ± 0.08)
excited state, pK_a*	2.82 (3.00 ± 0.03)	3.89 (4.07 ± 0.05)	2.85 (2.72 ± 0.06)

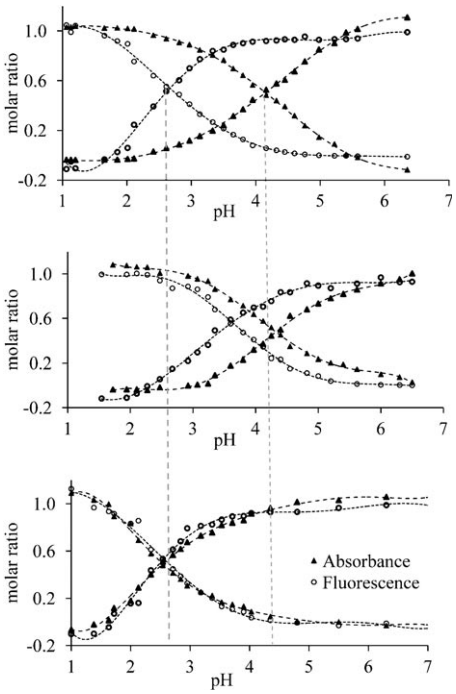

Figure 10. Calculated molar ratio for each of the components as a function of pH using PCA. The intersection of the two molar ratio curves corresponds to the pK_a of the protolytic equilibrium.

values. The intersections of absorption curves correspond to the pK_a in the ground state, whereas intersections of the fluorescence curves correspond to the pK_a in the excited state. The top panel describes the equilibrium between the neutral imidazole **2** and its protonated form **2H$^+$** (**2**↔**2H$^+$**). Clearly, the intersections of absorptions and fluorescence differed. The pK_a found for the excited state (pK_a*=2.82) was markedly lower than that in the ground state (pK_a= 4.20), indicating photoacidic properties. The same approach for imidazole **4H$^+$** revealed substantially less photoacidity than **2H$^+$** and negligible photoacidity for compound **5H$^+$**.

The results shown in Figure 10 clearly illustrate which nitrogen in the imidazole ring is responsible for the pH sensitivity in the ground and excited states. The dissociation constants of **2H$^+$** in the ground state were identical to the dissociation constant of **4H$^+$** (dashed vertical line on the right-hand side) in the ground state, suggesting similar mechanisms of protonation/deprotonation. Indeed, it is generally accepted that the 3-N position in imidazoles is preferably protonated under acidic conditions due to the lone electron pair localized on the 3-N position.[30] The unshared electron pairs in **2** and **4**, which are localized on the 3-N position, are equally available for protonation and thus apparently have similar basicity as indicated by their identical pK_a values, which suggests the isoelectronic configuration of **2H$^+$** and **4H$^+$** in the ground state. In contrast to the ground state, the excited state of imidazole **4H$^+$** showed substantially higher basicity (pK_a* 3.87) than **2H$^+$** in its excited state (pK_a* 2.82), demonstrating the divergence of their electronic configurations in the excited state. In contrast, the dissociation constants in the excited states of **2H$^+$** and 3-*N*-Me **5H$^+$** (pK_a* 2.85) were nearly identical, suggesting *isoelectronic configurations of* **2H$^+$** *and* **5H$^+$** in their excited states. Thus, imidazole **2H$^+$** is similar to **4H$^+$** in the ground state and **5H$^+$** in the excited state.

To explain this phenomenon, we propose a mechanism based on excited-state charge transfer, where the rearrangement in electron density upon excitation leads to a swap of a positive charge between 1-N to 3-N. Upon excitation, the electron density in the imidazole ring rearranges in such a way so that the positive charge moves from the 3-N position in the ground state to the 1-N position in the excited state, as shown in a modified Förster cycle (Scheme 3). In this scheme, the ground state **2H$^+$** resembles the ground state of **4H$^+$** (as shown by a double-headed arrow) and the excited state **2H$^+$** resembles **5H$^+$** (as shown by a double-headed arrow). Upon excitation, the redistribution of charges in **2H$^+$** takes place, resulting in a shift of electron density from one nitrogen to another.

Conclusions

An imidazole incorporated into a fluorophore showed a wealth of pH-dependent optical properties. Investigation into the mechanisms of pH sensitivity was accomplished by synthesizing the mono- and di-*N*-methylated analogues and provided the following findings: 1) Fluorescent imidazole was found to be pH-sensitive in all three ranges of the pH scale from 2.0 to 11.0. Three distinct absorption bands at 360, 430, and 477 nm in acidic, neutral and basic conditions were assigned to the protonated, neutral, and deprotonated forms of imidazole. The deprotonotated and neutral forms of fluorescent imidazole emitted at 530 and 560 nm correspondingly; in acidic conditions, the emission shifted to 600 nm. 2) 1-N was determined to be a pH-sensitive center in the ground state, whereas 3-N was responsible for pH sensitivity in the excited state. Such switching between the centers was attributed to the excited-state charge transfer (ESCT) from one nitrogen to another, resulting in a positive charge swapping between two nitrogens. 3) pK_a analysis in the ground and the excited state showed photoacidic properties of the studied fluorescent imidazole, which were attributed to excited-state proton transfer (ESPT); this effect was found negligible for substituted imidazoles and under basic conditions. 4) Large Stoke shifts of the dyes in protonated form and much shorter Stokes shift in the deprotonated form clearly indicate the presence of pH-dependent twisted

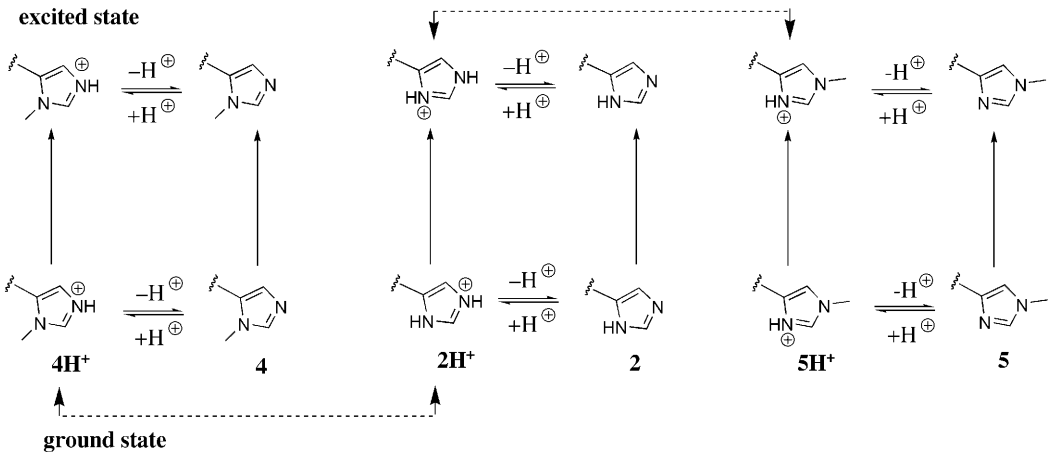

Scheme 3. Proposed Förster cycle for imidazole compounds, illustrating the similarity between **2H$^+$** and **4H$^+$** in the ground state and between **2H$^+$** and **5H$^+$** in the excited state.

intramolecular charge transfer (TICT). The mechanism of this channel as well as theoretical experimental data confirming the presence of the process will be the focus of further study.

Experimental Section

General procedure for conjugating imidazolecarbaldehydes to benzo[*e*]indolium: To imidazole carbaldehyde (1.0–1.1 equiv) in methanol, 3-(2-carboxyethyl)-1,1,2-trimethyl-1*H*-benzo[*e*]indolium **1**[31] bromide (1.0 equiv) was added, followed by the addition of sodium acetate (1.5 equiv). The reaction mixture was stirred for 20 h at room temperature in the dark. The final product was isolated by using reversed-phase, medium-pressure flash chromatography (Biotage AB, Sweden) with a gradient 10%–95% acetonitrile in water (both solvents contained TFA (0.1%)). NMR spectra were recorded on 300 MHz GE Omega and on 600 MHz Varian NMR spectrometers. LC/MS-ESI analysis in the positive mode was conducted on a Shimadzu LCMS 2010 A equipped with a UV/Vis and fluorometer detector using a reversed-phase C-18 column.

Optical measurements: UV/Vis spectra of samples predissolved in methanol and diluted with water were recorded by using a Beckman-Coulter DU-640 spectrophotometer. Fluorescence spectra were recorded by using a Fluorolog III (Horiba Jobin Yvon Inc., Edison NJ) fluorometer using excitation at 400 nm unless indicated. Quantum yields of species at acidic and neutral pH (excitation 400 nm) were recorded referenced to quinine hemisulfate monohydrate in 0.1 M H_2SO_4 in water ($\Phi = 0.54$[32]); for basic species (excitation 460 nm) quantum yield was recorded referenced to fluorescein in 0.1 N NaOH in water ($\Phi = 0.95$.[32]). The fluorescence lifetime was measured by using the time-correlated single-photon counting (TCSPC) technique (Horiba) with excitation sources NanoLed 370 and 460 nm and a R928P detector (Hamamatsu Photonics, Japan) set to 600 nm or 560 nm, respectively. The instrument response function was obtained by using the Rayleigh scatter of Ludox-40. DAS6 v6.1 decay analysis software (Horiba) was used for the lifetime calculations.

Titration experiments: Compounds **2–5** were dissolved in methanol (0.2 mL) and added into a beaker with water (100 mL) under stirring. A flow of argon was constantly delivered to the top of the solution to keep CO_2 out. The solution was basified with dilute aqueous NaOH, and the desired pH was attained by titrating with aqueous HCl, or backwards at relatively low ionic strengths ($I = 0.02$–0.05 M). The pH of the solution was continuously measured by using an Accumet pH meter AB15 (Fisher Sci.). The pK_a values were calculated by using principal component analysis software (DATAN 3.1, MultiD Analyses AB, Sweden) and a sigmoidal dose-response curve fit implemented in the software Prism 5.0 (GraphPad Software Inc., La Jolla, CA).For optical measurements in glycerol, compound **2** was pre-dissolved in methanol, and the methanolic solution (10 uL) was added to cuvettes with neutral and acidic glycerol (1 mL) (acidified with TFA, total volume of TFA 0.06 vol%). The glycerol solutions were stirred with a small spatula directly in a cuvette and allowed to stand for 2 h in the dark for complete homogenation.

Acknowledgements

We thank Dr. Yunpeng Ye for providing 3-(2-carboxyethyl)-1,1,2-trimethyl-1*H*-benz[*e*]indolium bromide, and Prof. Vladimir Birman for fruitful discussions. This study was supported in part by the NIH (NIBIB R01 EB7276).

[1] S. Charier, O. Ruel, J. B. Baudin, D. Alcor, J. F. Allemand, A. Meglio, L. Jullien, B. Valeur, *Chem. Eur. J.* **2006**, *12*, 1097–1113.
[2] O. Finikova, A. Galkin, V. Rozhkov, M. Cordero, C. Hagerhall, S. Vinogradov, *J. Am. Chem. Soc.* **2003**, *125*, 4882–4893.
[3] P. Herman, H. Drapalova, R. Muzikova, J. Vecer, *J. Fluoresc.* **2005**, *15*, 763–768.
[4] Z. Zhang, S. Achilefu, *Chem. Commun.* **2005**, 5887–5889.
[5] S. Ikeda, A. Okamoto, *Photochem. Photobiol. Sci.* **2007**, *6*, 1197–1201.
[6] O. Shimomura, *FEBS Lett.* **1979**, *104*, 220–222.
[7] H.-w. Ai, N. C. Shaner, Z. Cheng, R. Y. Tsien, R. E. Campbell, *Biochemistry* **2007**, *46*, 5904–5910.
[8] X. Shu, N. C. Shaner, C. A. Yarbrough, R. Y. Tsien, S. J. Remington, *Biochemistry* **2006**, *45*, 9639–9647.
[9] R. Y. Tsien, *Annu. Rev. Biochem.* **1998**, *67*, 509–544.
[10] K. Nienhaus, G. U. Nienhaus, J. Wiedenmann, H. Nar, *Proc. Natl. Acad. Sci. USA* **2005**, *102*, 9156–9159.
[11] J. Dong, K. M. Solntsev, O. Poizat, L. M. Tolbert, *J. Am. Chem. Soc.* **2007**, *129*, 10084–10085.
[12] N. C. Shaner, P. A. Steinbach, R. Y. Tsien, *Nat. Methods* **2005**, *2*, 905–909.
[13] N. C. Shaner, R. E. Campbell, P. A. Steinbach, B. N. Giepmans, A. E. Palmer, R. Y. Tsien, *Nat. Biotechnol.* **2004**, *22*, 1567–1572.
[14] J. Catalan, J. C. Delvalle, R. M. Claramunt, G. Boyer, J. Laynez, J. Gomez, P. Jimenez, F. Tomas, J. Elguero, *J. Phys. Chem.* **1994**, *98*, 10606–10612.
[15] V. Jimenez, J. B. Alderete, *J. Mol. Struct.* **2006**, *779–800*, 1–7.
[16] J. Wierzchowski, J. Sepiol, D. Sulikowski, B. Kierdaszuk, D. Shugar, *J. Photochem. Photobiol. A* **2006**, *179*, 276–282.
[17] M. Y. Berezin, S. Achilefu, *Tetrahedron Lett.* **2007**, *48*, 1195–1199.
[18] P. Benjes, R. Grimmett, *Heterocycles* **1994**, *37*, 735–738.
[19] G. Shapiro, B. Gomez-Lor, *J. Org. Chem.* **1994**, *59*, 5524–5526.
[20] T. Mohammad, H. Morrison, H. HogenEsch, *Photochem. Photobiol.* **1999**, *69*, 115–135.
[21] In compound **4**, fast H/D exchange in [D_4]MeOH precluded the observation of NOEs between H-11 and H-14, which would be a direct proof of *trans–cis* conformation in **4**. In compound **5** the H/D exchange was insignificant and the absence of NOEs between H-11 and H-14 confirmed the *trans–trans* conformation of **5.**
[22] J. Catalan, P. Cabildo, J. Elguero, J. Gomez, J. Laynez, *J. Phys. Org. Chem.* **1989**, *2*, 646–652.
[23] H. Walbe, R. W. Isensee, *J. Org. Chem.* **1956**, *21*, 702–704.
[24] Y. Odo, K. Matsuda, M. Irie, *Chem. Eur. J.* **2006**, *12*, 4283–4288.
[25] C. Geddes, J. Lakowicz, *Advanced Concepts in Fluorescence Sensing Part A: Small Molecule Sensing*, Springer, Heidelberg, **2005**, p. 328.
[26] N. Agmon, *J. Phys. Chem. A* **2005**, *109*, 13–35.
[27] T. Forster, *Z. Elektrochem.* **1950**, *54*, 531–535.
[28] L. M. Tolbert, K. M. Solntsev, *Acc. Chem. Res.* **2002**, *35*, 19–27.
[29] P. Wan, D. Shukla, *Chem. Rev.* **1993**, *93*, 571–584.
[30] A. L. Lehninger, D. L. Nelson, M. M. Cox, *Principles of Biochemistry*, Worth Publishers, New York, **1993**, p. .
[31] Y. Ye, W. P. Li, C. J. Anderson, J. Kao, G. V. Nikiforovich, S. Achilefu, *J. Am. Chem. Soc.* **2003**, *125*, 7766–7767.
[32] J. R. Lakowicz, *Principles of fluorescence spectroscopy*, Springer, New York, **2006**, p. 954 S.
[33] www.jobinyvon.com/SiteResources/Data/MediaArchive/files/Fluorescence/applications/quantumyieldstrad.pdf.

Received: August 29, 2008
Revised: December 18, 2008
Published online: February 11, 2009

